

Radiative Flux Analysis (RADFLUXANAL) Value-Added Product: Retrieval of Clear-Sky Broadband Radiative Fluxes and Other Derived Values

LD Riihimaki
CN Long

KL Gaustad

September 2019



DISCLAIMER

This report was prepared as an account of work sponsored by the U.S. Government. Neither the United States nor any agency thereof, nor any of their employees, makes any warranty, express or implied, or assumes any legal liability or responsibility for the accuracy, completeness, or usefulness of any information, apparatus, product, or process disclosed, or represents that its use would not infringe privately owned rights. Reference herein to any specific commercial product, process, or service by trade name, trademark, manufacturer, or otherwise, does not necessarily constitute or imply its endorsement, recommendation, or favoring by the U.S. Government or any agency thereof. The views and opinions of authors expressed herein do not necessarily state or reflect those of the U.S. Government or any agency thereof.

Radiative Flux Analysis (RADFLUXANAL) Value-Added Product: Retrieval of Clear-Sky Broadband Radiative Fluxes and Other Derived Values

LD Riihimaki, Cooperative Institute for Research in Environmental
Sciences (CIRES)
KL Gaustad, Pacific Northwest National Laboratory
CN Long, CIRES (Retired)

September 2019

Work supported by the U.S. Department of Energy,
Office of Science, Office of Biological and Environmental Research

Executive Summary

This technical report describes the algorithms used in the Radiative Flux Analysis (RADFLUXANAL) Value-Added Product (VAP). This VAP estimates clear sky broadband irradiance values and derives several additional cloud properties from broadband measurements including fractional sky cover and cloud optical depth. The VAP is based on a collection of algorithms and codes developed by Charles N. Long. It is an updated version of the Shortwave Flux Analysis VAP that has been used in ARM for a number of years. The RADFLUXANAL VAP includes two major updates over the previous Shortwave Flux Analysis VAP: 1) longwave (LW) clear sky irradiance estimates and derived parameters, and 2) takes in better quality-controlled input data from the QCRAD VAP.

Acronyms and Abbreviations

ARM	Atmospheric Radiation Measurement
ASI	Ascension Island
BRS	broadband radiometer station
BSRN	Baseline Surface Radiation Network
CFI	cloud-free index
CLOWD	Clouds with Low Optical Water Depths
ENA	Eastern North Atlantic
FKB	Black Forest, Germany
GAN	Gan Island, Maldives
GNDRAD	ground radiometers on stand for upwelling radiation
GRW	Graciosa Island, Azores
HFE	Shouxian, China
IRT	infrared thermometer
LDR	longwave downward radiation
LW	longwave
MAO	Manacapuru, Brazil
MET	surface meteorological instrumentation
NIM	Niamey, Niger
NSA	North Slope of Alaska
OKI	Oliktok Point
PCA	partial cloud amount
PSP	precision spectral pyranometer
PVC	Cape Cod, Massachusetts
PYE	Point Reyes, California
QCRAD	Data Quality Assessment for ARM Radiation Data value-added product
RADFLUXANAL	Radiative Flux Analysis value-added product
SGP	Southern Great Plains
SIRS	solar and infrared radiation station
SKYRAD	sky radiometers on stand for downwelling radiation
SURFRAD	Surface Radiation Budget Network
SW	shortwave
SWCLRID	Shortwave Clear-Sky Detection and Fitting algorithm
TWP	Tropical Western Pacific
TWP-ICE	Tropical Warm Pool–International Cloud Experiment
VAP	value-added product
WMO	World Meteorological Organization

Contents

Executive Summary	iii
Acronyms and Abbreviations	iv
1.0 Introduction	1
2.0 Input Data	1
3.0 Output Data	1
4.0 Algorithm Descriptions	2
4.1 SW Clear-Sky Estimates	3
4.1.1 Identifying Clear-Sky Periods	3
4.1.2 Estimating Clear-Sky Irradiance: Daily Fit versus One-Fit-for-All Mode.....	4
4.1.3 Iterating to Find the Best Fit.....	5
4.1.4 Estimating Clear-Sky Upwelling SW.....	6
4.2 SW Derived Parameters	7
4.2.1 SW Fractional Sky Cover.....	7
4.2.2 SW Cloud Optical Depth.....	8
4.3 LW Clear-Sky Estimates	9
4.3.1 Identify LW Effective Clear-Sky Periods	10
4.3.2 Use Data to Fit Coefficients for Brutsaert Formula	10
4.3.3 Interpolate for Cloudy Periods and Estimate Continuous Clear-Sky Downwelling LW.....	10
4.4 LW Derived Parameters	11
4.4.1 LW Fractional Sky Cover	11
4.4.2 Cloud Radiating Temperature	12
5.0 Future Work.....	13
6.0 References	14

Figures

1	Flow chart of iterations between clear-sky identification, clear-sky fitting, and coefficient interpolation.....	6
2	Normalized Diffuse Cloud Effect (D_n) versus fractional sky cover at Table Mountain SURFRAD site.	7
3	Look up table describing decision tree for LW fractional sky cover.	12
4	Example of cloud temperature derived from broadband LW measurements (red line) in the RADFLUXANAL VAP compared to the infrared thermometer (blue, IRT_{avg}).....	13

Tables

1	Calculated output variables in RADFLUXANAL.	2
2	Mode used to run RADFLUXANAL VAP at all currently processed sites.	5

1.0 Introduction

The Radiative Flux Analysis (RADFLUX) is a technique for using surface broadband radiation measurements for detecting periods of clear (i.e., cloudless) skies, and using the detected clear-sky data to fit functions that are then used to produce continuous clear-sky estimates. The clear-sky estimates and measurements are then used in various ways to infer cloud macrophysical properties.

This value-added product (VAP) is based on methodologies developed by Dr. Charles N. Long as referenced in the papers below. It is an updated version of an earlier value-added data product called the Shortwave (SW) Clear-Sky Detection and Fitting Algorithm (SWCLRID). Two major improvements were made over the SWCLRID data product: 1) input data were first run through the Data Quality Assessment for Atmospheric Radiation Measurement (ARM) Radiation Data (QCRAD) VAP to better screen for data quality, and 2) additional processing was implemented to also include longwave (LW) clear sky estimates and derived values.

2.0 Input Data

The required input data for these codes are broadband SW and LW radiative fluxes, including SW direct and diffuse components, and surface air temperature and humidity. These variables and additional variables such as wind speed and infrared thermometer (IRT) data are used for automated quality control in the QCRAD VAP (Long and Shi 2006, 2008), which applies various climatological and data comparison tests to identify common errors in radiative flux measurements. QCRAD also calculates the highest-quality total downwelling SW variable as recommended by the World Meteorological Organization (WMO) Baseline Surface Radiation Network (BSRN). First it applies a correction to precision spectral pyranometer (PSP) measurements of downwelling total SW to account for infrared loss (Dutton et al. 2001, Younkin and Long 2003). Then a best estimate total SW variable is created consisting of the sum of direct and diffuse irradiance measurements when available and filling in with PSP measurements as a backup.

All input data for the RADFLUXANAL VAP are taken from the QCRAD datastream, though the original datastreams that feed into QCRAD include the solar and infrared radiation station (SIRS), broadband radiometer station (BRS), or sky radiometers on stand for downwelling radiation (SKYRAD)/ground radiometers on stand for upwelling radiation (GNDRAD), surface meteorological instrumentation (MET), and IRT.

3.0 Output Data

In addition to carrying through upwelling and downwelling SW and LW fluxes, a number of additional parameters are calculated in the RADFLUXANAL VAP. The main measured and calculated parameters are listed in Table 1 below, with references for the algorithms of calculated parameters given in the final column (discussed further in Section 4).

Table 1. Calculated output variables in RADFLUXANAL.

Variable Name	Definition	Units	Reference
downwelling_shortwave	best estimate downwelling SW from sum or global pyranometer	W/m ²	From QCRAD; Long and Shi, (2006), Long and Shi (2008)
clearsky_downwelling_shortwave	estimated clear-sky downwelling SW	W/m ²	Long and Ackerman (2000)
clearsky_downwelling_longwave	estimated clear-sky downwelling LW	W/m ²	Brutsaert (1975), Long and Turner (2008)
clearsky_upwelling_shortwave	best estimate downwelling SW from sum or global pyranometer	W/m ²	Long (2005)
clearsky_upwelling_longwave	estimated clear-sky upwelling LW (W/m ²)—note: only measured upwelling LW is included when LW is clear	W/m ²	Long and Turner (2008); Long (2005)* method currently not implemented
clearsky_diffuse_downwelling_shortwave	estimated clear-sky downwelling diffuse SW (W/m ²)	W/m ²	Long and Ackerman (2000)
clearsky_direct_downwelling_shortwave	estimated clear-sky downwelling diffuse SW (W/m ²)	W/m ²	Long and Ackerman (2000)
clearsky_status	Clear sky flag: 1 if SW detected clear sky, 2 if LW detected, 9 if CLW>LW, 3 if only std and Ta-Te diff OK and ONLY LWup accepted as clear LWup [NOT LWdn!!!], else 0 if cloudy	Flag--none	Long and Ackerman (2000)
cloudfraction_longwave	estimated effective LW fractional sky cover	unitless	Durr and Philipona (2004), Long (2004)
cloudfraction_shortwave	estimated fractional sky cover from SW	unitless	Long et al. (2006)
visible_cloud_optical_depth	estimated effective visible cloud optical depth (only for SWScv>0.95)	unitless	Barnard et al. (2008)
brightness_temperature	Sky brightness temp from LWdn	K	LW = Sigma*T ⁴
cloud_radiating_temperature	estimated effective cloud radiating temperature	K	Unpublished—considered experimental, use with caution
cloud_transmissivity_shortwave	estimated effective SW cloud transmissivity (SWdn/CSWdn ratio)	unitless	Long and Ackerman (2000)
clearsky_emissivity_longwave	effective clear-sky LW emissivity	unitless	(Long, 2004; Long and Turner, 2008)

4.0 Algorithm Descriptions

Various portions of the Radiative Flux Analysis methodology are described in Long and Ackerman (2000), Long and Gaustad (2004), Long (2004, 2005), Long et al. (2006), Long and Turner (2008), Barnard and Long (2004), and Barnard et al. (2008). The clear-sky LW and LW effective sky cover techniques are based on the pioneering work of Marty and Philipona (2000) and Durr and Philipona, (2004), which in turn use a formulation from Brutsaert (1975).

Note there are two additional calculations in C.N. Long's Radiative Flux Analysis that were deemed experimental and we chose not to include them in this VAP. Calculated upwelling LW clear-sky calculations (Long 2005) were not included. Instead, only measured upwelling clear-sky values were used when the downwelling LW was determined to be effectively clear and clear-sky LW is otherwise labeled missing. An experimental calculation interpolating upwelling clear-sky LW is available in Chuck Long's original code, but is not included in the VAP. Cloud height estimates were also not included. One highly experimental value that was included is cloud radiating temperature. This is a step towards the calculation for cloud height but depends on fewer assumptions, so is considered slightly better known. Initial tests show that it matches IRT values well when LW fractional sky cover is greater than 0.5; however, the method has not yet been published in peer-reviewed literature and should be used with caution.

The algorithms used to calculate SW clear-sky estimates, derived SW parameters, LW clear-sky estimates, and derived LW parameters are summarized in the remainder of Section 4 for convenience, though data users are referred to the cited publications for more thorough descriptions of the algorithms and their evaluation.

4.1 SW Clear-Sky Estimates

The article by Long and Ackerman (2000) describes the first step in the Radiative Flux Analysis processing, where clear-sky downwelling SW measurements are identified, a clear-sky curve is empirically fit to the measurements, and downwelling clear-sky SW irradiance is estimated for all cloudy periods. Detailed instructions for running the codes that calculate SW clear-sky estimates and derived parameters are given in Long and Gaustad (2004) and will not be repeated here. Instead, this report will summarize the algorithms used for calculating these parameters, and provide insight into how to use them accurately for analysis.

4.1.1 Identifying Clear-Sky Periods

Four tests are used to identify clear-sky periods (Long and Ackerman 2000), based on the magnitude and variability of the total and diffuse irradiance normalized by the cosine of the solar zenith angle.

- Normalized Total Shortwave Magnitude Test:** The first test checks for limits on the magnitude of the total downwelling SW irradiance normalized by a power-law function of the cosine of the solar zenith angle. That is, the normalized total downwelling SW irradiance (F_N) is defined as $F_N = F_{\downarrow} / \mu_o^{b_{tot}}$ where F_{\downarrow} is the downwelling irradiance, μ_o is the cosine of the solar zenith angle, and b is a constant that is fit to the data empirically. Normalization by the cosine of the zenith angle removes much of the diurnal cycle of the SW irradiance, allowing separation of changes in magnitude of the irradiance due to the impact of clouds from that of solar geometry. Thresholds on the magnitude of the normalized total shortwave are used as a first test to eliminate cloudy periods.
- Maximum Diffuse Shortwave Test:** Under cloudy skies the diffuse irradiance increases as more incident radiation is scattered from the direct beam. So, a maximum diffuse limit (D_{lim}) is also used to screen out cloudy periods, defined as $D_{lim} = D_{max} \mu_o^{0.5}$. D_{max} is a constant set in the configuration file, and the limit is once again a function of the cosine of the zenith angle to account for the variability in the solar cycle.

- **Change in Magnitude with Time Test:** Optically thin clouds and partially cloudy skies may not change the magnitude of the total or diffuse irradiance enough in an individual measurement to be identified with the magnitude tests, so variability criteria are important for catching all cloudy conditions. Under cloudy conditions the total irradiance is more variable from minute to minute than under clear-sky conditions. Thus, a third test sets a maximum and minimum limit on the change in total irradiance per minute ($|\Delta F_{\downarrow}/\Delta t|$). In order to account for the variability caused by solar geometry, these limits are based on the variability of the solar irradiance incident at the top of the atmosphere ($|\Delta F_{\downarrow T}/\Delta t|$). The max and min limits for the 1-minute resolution data used by ARM are set as follows, where C is a subjective constant set in the configuration file incorporating the noise of the instruments:

$$MAX = |\Delta F_{\downarrow T}/\Delta t| + C\mu_o$$

$$MIN = |\Delta F_{\downarrow T}/\Delta t| - (\mu_o^{noon} + 0.1)/\mu_o$$

- **Normalized Diffuse Ratio Variability Test:** The final test looks at the variability of the ratio between the diffuse and total downwelling SW irradiance. This is the most sensitive test because it can detect subtle changes that shift either the direct or diffuse irradiance with time since it contains both components implicitly in the total irradiance. A threshold is set on the standard deviation of the normalized diffuse ratio, such that $\sigma(D_N) < Limit$. The normalized diffuse ratio defined as $D_N = D_{\downarrow}/\mu_o^{b_{dif}}$, where b_{dif} is a constant that is fit to the data empirically. The *Limit* threshold is a subjective constant given in the configuration file that is generally set to 0.0012 for an 11-minute period based on examination of data in the field.

4.1.2 Estimating Clear-Sky Irradiance: Daily Fit versus One-Fit-for-All Mode

The RADFLUX analysis identifies clear periods and estimates clear-sky SW irradiance using empirical fits to those clear periods. Fits are performed using least squares regression in order to fit both the total downwelling SW irradiance and the diffuse ratio in an equation of the form: $Y = a\mu_o^b$, where Y is either the total SW irradiance or the diffuse ratio, and a and b are regression coefficients.

Interpolation of the empirical fit coefficients is used to estimate clear-sky SW irradiance on days with insufficient clear periods for a fit. This is done in two ways depending on how cloudy the site is.

In climates characterized by semi-frequent clear-sky conditions, the clear-sky fit coefficients are calculated for each “clear enough” day as defined by Long and Ackerman (2000), and linearly interpolated for cloudy periods. The algorithm stores the coefficients from the last day in the data run that had enough clear measurements to be fitted; thus files from time periods immediately following the data run can be processed and coefficients interpolated between this “last day” and the first day of the new run that has sufficient clear-sky measurements for fitting. A “clear enough day” is defined as a day for which at least the minimum number of points as set in the configuration file (usually set to 110) were found to be clear, and these points encompassed a sufficient range of that day’s possible solar zenith angle. Further details are available in Long and Ackerman (2000).

To produce a continuous estimate of clear-sky shortwave irradiance in climates that infrequently have clear-sky conditions, a single set of clear-sky coefficients are calculated for the entire run rather than a series of daily coefficients. For the total downwelling SW, the one-fit estimates, if adjusted for Earth-Sun

distance, do almost as well as the daily fit mode. However, the diffuse and direct component clear-sky estimates do not fare so well using only one set of coefficients. This is because skies may be determined as “clear”, but may have differences in haze or aerosol amounts. In these cases, the haze acts to repartition the energy from the direct component, but still scatter the vast majority of the energy in the forward direction, thus including it in the diffuse portion. For all intents and purposes, the total remains the same. The one-fit-for-all mode, after the final “normal” iteration, goes back through the data a final time looking for minimum occurrences of the normalized diffuse ratio for CosZ greater than the limit set in the configuration file. More details on this method are given in Long and Gaustad (2004). Table 2 shows whether daily fit or one-fit mode was used at the sites that have currently been processed. A global attribute (fitmode) in the RADFLUXANAL VAP files also tells which mode was used to process that file.

Table 2. Mode used to run RADFLUXANAL VAP at all currently processed sites.

Site	Daily/One Fit
SGP—All Facilities	Daily
TWP C1, C2 (Manus, Nauru)	One Fit
TWP C3 Darwin, Australia	During the dry season Daily mode is run, but one fit mode is used during the monsoon season when much cloudier.
NSA C1 Barrow, Alaska	Daily mode
ENA C1 Azores, Portugal	One Fit
ASI, Ascension Island	One Fit
FKB, Black Forest Germany	Daily mode
GAN, Gan Island, Maldives	Daily mode
GRW, Azores, Portugal	One Fit
HFE, Shouxian, China	Daily mode
MAO, Manacapuru, Brazil	One Fit
NIM, Niamey, Niger	Daily mode
OLI, Oliktok Point, Alaska	Daily mode
PVC, Cape Cod, Massachusetts	Daily mode
PYE, Pt Reyes, California	Daily mode

4.1.3 Iterating to Find the Best Fit

The clear-sky identification, empirical clear-sky fits, and interpolation are performed iteratively to sequentially improve the clear-sky fits. More details are given in Long and Ackerman (2000), but we reproduce the flow chart from that paper below for an overview of the iterative process.

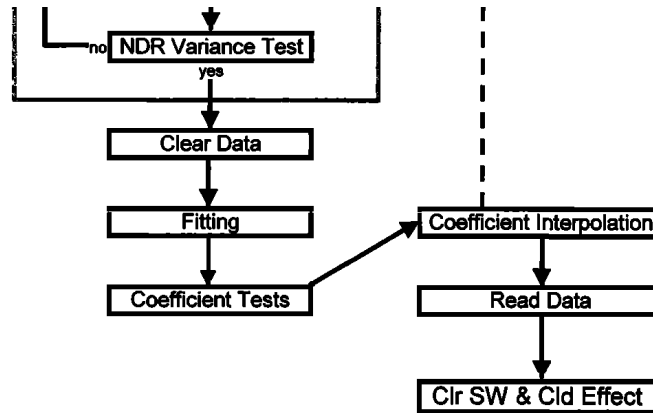


Figure 16. Flowchart for the automated clear-sky identification and fitting algorithm. NSW, normalized total shortwave irradiance; dif SW, diffuse shortwave irradiance; del TSW, change in total shortwave irradiance; NDR, normalized diffuse ratio; Clr SW, clear-sky shortwave irradiance; cld effect, downwelling shortwave cloud effect.

data sampling rate. The total shortwave standard deviation from $x = y$ for both clear and cloudy sky converges to a value of $\sim 20 \text{ Wm}^{-2}$ with averaging of 30 min or longer (C. N. Long, unpublished internal report, 1996). Despite these differences

Figure 1. Flow chart of iterations between clear-sky identification, clear-sky fitting, and coefficient interpolation. Figure taken from Long and Ackerman (2000).

4.1.4 Estimating Clear-Sky Upwelling SW

Clear periods identified from downwelling SW measurements are also applied to find upwelling SW clear measurements. However, there are additional challenges estimating upwelling SW measurements using only detected clear-sky measurements, and then interpolating fit coefficients as we do for the downwelling SW (Long 2005). For instance, when it snows, it is cloudy; thus the "fit" is not good until the next "clear enough" day for fitting after the snow event. This introduces a large error during the period, and for times of snow melt. Data show that the bi-directional reflectance function also changes over time depending on the surface characteristics. Thus, the current procedure for estimating clear-sky upwelling SW is to look through the data and take a daily average for all data from 1100 through 1300 local standard time. This captures, at least on a daily basis, the major changes in surface albedo such as those from snow accumulation or snow melt. A second pass through the data then uses the "daily noon average" as a constant, and determines a function for any data that include at least 25% of the total SW produced by the direct component (i.e., significant direct sunlight producing the bi-directional nature of the albedo dependence) using the cosine of the solar zenith angle as the independent variable. Again, these fit coefficients are interpolated for days when insufficient direct SW data are available for fitting. The function is then multiplied times the estimated clear-sky SW_{dn} to produce a continuous estimate of clear-sky SW_{up}. Examination of these results so far suggests that this technique generally eliminates the poor fit due to the sky being cloudy when it snows, and does a better job than just multiplying the measured albedo (SW_{up}/SW_{dn}, which often behaves erratically through time depending on whether the direct sun is blocked by cloud or not) times the clear-sky SW_{dn}.

4.2 SW Derived Parameters

4.2.1 SW Fractional Sky Cover

Fractional sky cover is inferred from measured and clear-sky downwelling SW irradiances for solar elevation angles greater than 10° using the method described in Long et al. (2006). The algorithm was developed using empirical fits to total sky imager data and is valid for an effective 160° field of view.

The technique is based on the fact that the diffuse irradiance increases with increased cloud cover. The primary variable used to determine the fractional sky cover is the Normalized Diffuse Cloud Effect: $D_n = [\text{Dif} - \text{Cdif}]/\text{CSW}$, plotted in Figure 2. In general, fractional sky cover (FSC) is determined using the equation $FSC = 2.255(D_n)^{0.9381}$ (Figure 2, black line) but additional tests are done to identify overcast cases with a larger range of D_n values.

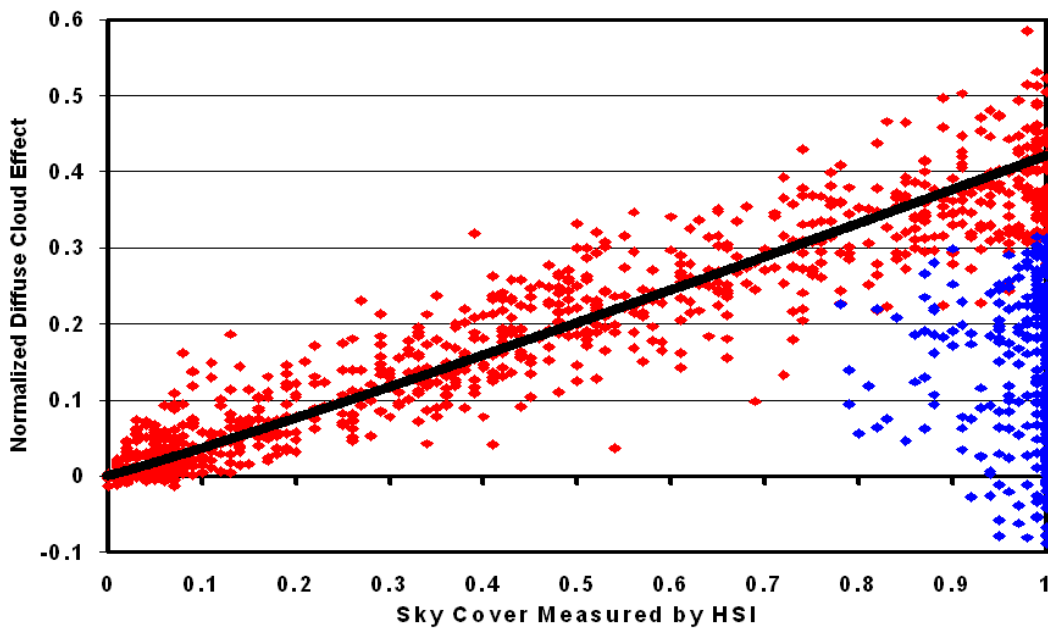


Figure 2. Normalized Diffuse Cloud Effect (D_n) versus fractional sky cover at Table Mountain SURFRAD site. Black line shows fit used to calculate sky cover from Normalized Diffuse Cloud Effect. Red-circled regions show two types of cases when D_n is negative. Blue points indicate overcast cases identified using additional tests. Based on Figure 3 of Long et al. (2006).

First, negative D_n values can come from clear or optically thick overcast conditions (see Figure 2, red-circled areas) and are separated using an effective transmissivity (total downwelling SW/clear downwelling SW) threshold of 0.4. Optically thick clouds have a small transmissivity as they block more incoming radiation, while clear skies have a transmissivity around 1. An additional test is applied to D_n between 0 and 0.37, to identify thick overcast cases (Figure 2, blue points): when the average diffuse ratio (diffuse/total) is 90% or greater, and the 15-min standard deviation of the diffuse ratio is less than 0.05, the points are considered overcast. This is based on the fact that optically thick overcasts scatter all incoming radiation (diffuse ratio close to 100%), and give relatively uniform irradiance over time (small standard deviation).

Additionally, points determined clear by the Long and Ackerman (2000) method are assigned a fractional sky cover of zero.

Since these clear-sky and overcast conditions use thresholds that can cause the retrieved fractional sky cover to vary artificially compared to the time scale of change in the atmosphere, additional tests are applied to 11-minute periods that are nearly clear or nearly overcast to better smooth the results.

- Nearly overcast: For an 11-minute window around a given point, substitute value from the offset and slope fit to those 11 points using the MEDFIT fitting routine (Press et al. 1986) that removes outliers, when these criteria are met:
 1. at least one value in 11-minute running window is set to overcast,
 2. if data point is more than 1 absolute deviation from 11-pt mean, and
 3. if absolute difference between data point and mean is greater than 0.04 sky cover.
- Nearly clear: (Note this method is updated from Long et al. 2006). For an 11-minute window around a given point, substitute the 11-point running average when the following conditions are met:
 1. at least 70% of 11 points are set to clear window are being set by the empirical fit equation, and
 2. at least one data point is set to zero sky cover by either the Long and Ackerman (2000) method or because $D_n < 0$, and
 3. less than 3 points are set to clear by the clear identification algorithm of Long and Ackerman (2000).

4.2.2 SW Cloud Optical Depth

The cloud optical depth estimates are based on a technique by Barnard et al. (2008). This technique, a derived relationship based on the results of Min and Harrison (1996) and Min et al. (2004), is officially only valid for overcast skies (sky cover > 0.90). Thus, the current output includes cloud optical depth only for sky cover > 0.90 for now. Also, comparisons conducted as part of the ARM Clouds with Low Optical Water Depths (CLOWD) project suggest that the Min and Harrison (1996) technique itself tends to overestimate the cloud optical depth for thinner clouds ($\tau < 5$) (Dave Turner, personal communication). Recent work using Tropical Warm Pool–International Cloud Experiment (TWP-ICE) data has prompted a change to using the total (global) SW in our formulation instead of the diffuse as in Min and Harrison, which appears to do well to compensate for this thin cloud overestimation (Barnard et al. 2008). The equation used to calculate cloud optical depth (τ) is:

$$\tau = \frac{\frac{1.16}{r} - 1}{(1 - A)(1 - g)}, \text{ where } r = \frac{T}{C\mu_o^{0.25}}$$

Here A =albedo, g = the asymmetry parameter, T =measured total SW, C =clear-sky total SW, and μ_o = cosine of the zenith angle.

Finally, an attempt is made to detect when the cloudiness present is likely to be ice clouds, for which an asymmetry parameter for ice (0.8 from Fu 1996) should be used rather than the standard 0.87 used for liquid water clouds. The sky brightness temperature calculated from the downwelling LW using the Stephan-Boltzman relationship (T_e) is compared to a limit temperature. The limit temperature is calculated using the effective clear-sky broadband LW emissivity (E_c) estimated by the Radiative Flux Analysis code (Long 2004, Long and Turner 2008; see Sections 4.3 and 4.4) and the assumption that $(1-E_c)$ is the extent to which clouds can influence the downwelling LW measurement. Then assuming a brightness temperature for the cloudy sky that contains a cloud at -40 C (where to first order only ice can exist), a limit is calculated as:

$$T_{lim} = \left(\frac{LW_{ice}}{\sigma}\right)^{0.25} - 2.0$$

$$LW_{ice} = LW_{clr} + scv(1 - E_c)\sigma T^4$$

Where LW_{ice} is the limit in terms of LW irradiance, LW_{clr} is the estimated clear-sky LW, scv is the fractional sky cover, σ is the Stephan-Boltzman constant, T is the cloudy-sky brightness temperature for a cloud at -40 C, and T_{lim} is the limit in terms of sky brightness temperature. Then for times with T_e is less than T_{lim} , an asymmetry parameter of 0.8 is used in the calculation of cloud optical depth; otherwise 0.87 is used. From analysis of ARM TWP-ICE data from Darwin, Australia, T_{ice} is set to 248 K to represent the ice cloudy sky brightness temperature.

4.3 LW Clear-Sky Estimates

The estimated clear-sky downwelling LW is derived from a technique based on Brutsaert (1975). Unlike the Brutsaert formulation, we use the known clear-sky periods and the corresponding measured clear-sky downwelling LW to calculate lapse rate coefficients. These calculated lapse rate coefficients are then interpolated for cloudy periods, similar to the SW technique. Comparisons show that about 80% of the estimated clear-sky LW falls within 4 W/m² of the corresponding clear-sky measured LW, and within 8 W/m² of radiative transfer calculations (which themselves agree with clear-sky measurements at the 4 W/m² level) used as a comparison under cloudy skies (Long and Turner 2008). There is a known "problem", however, in that the only information available for LW estimation is surface measurements. For those times of abrupt major changes in temperature or humidity profiles significantly differing from the data the lapse rate coefficients were determined from, such as cold front passages, the clear-sky LW estimates will exhibit greater error. This same problem occurs for model calculations due to the interpolation through time in between sonde profiles (Long and Turner 2008). Fortunately, these conditions occur infrequently.

A full description of the method used to estimate LW clear sky is given in Long and Turner (2008). There are three main steps in the calculation described in the sections below.

4.3.1 Identify LW Effective Clear-Sky Periods

Effective LW clear sky is identified in the data, where the clear sky is qualified as “effective” because high cold clouds often have no appreciable effect on the surface LW irradiance and so may be present when LW clear sky is included. Two criteria are used to identify LW effective clear skies, as described below:

1. *Smoothly varying atmosphere*: Under clear skies, the atmosphere changes slowly without the high temporal variability that clouds can bring. This physical mechanism is identified in the LW data using an upper limit on the standard deviation of downwelling LW over 21 minutes. The limit is set in the configuration file after manually examining the average of the largest 10% of the distribution of values during clear-sky periods detected using the SW technique (Long and Ackerman 2000).
2. *Sky brightness temperature is colder than atmospheric temperature*: Both uniform overcast and clear skies can give smoothly varying LW values, so the above criteria is not sufficient to identify clear periods. An additional threshold is set in the configuration file for the minimum difference between the measured 2-m atmospheric temperature and the effective sky brightness temperature. The effective sky brightness temperature is calculated using the Stephan-Boltzman equation. The threshold is set manually for a given site using the rule of thumb that the threshold is set to include the smallest 10% of values during SW detected clear-sky periods.

4.3.2 Use Data to Fit Coefficients for Brutsaert Formula

The effective clear sky LW irradiance (LW_c) is estimated using the Stephan-Boltzman equation with an adjustment for the effective clear-sky broadband emissivity (ϵ_c) as described by a formula from Brutsaert (1975): $LW_c \approx \epsilon_c \sigma T_a^4$, where T_a is the ambient air temperature, and σ is the Stephan-Boltzman constant. Brutsaert (1975) estimates the effective clear-sky broadband emissivity with the following equation: $\epsilon_c \approx C \left(\frac{e}{T_a}\right)^{1/7}$, where e is the vapor pressure in mbar and C is a constant that encompasses the temperature and humidity lapse rate information that impacts clear sky downwelling LW.

Brutsaert calculates C to be 1.24 for the U.S. standard atmosphere, but Long and Turner (2008) fit the coefficient based on known clear-sky data from the SW clear-sky identification. An additional factor is added for high-humidity cases to better separate haze from clouds. So the temperature and humidity lapse rate constant takes the form: $C = k + a(RH)^b$, where the power-law term is only used in high-humidity cases ($RH > 75-80\%$, depending on the site). The intent is to mimic the power-law behavior of how condensed water absorbs in the 8-12 um atmospheric window. A humidity of about 75% is used because it corresponds to the deliquescence point of salt crystals, meaning that haze drops would start to form in the presence of common cloud condensation nuclei at that humidity level.

4.3.3 Interpolate for Cloudy Periods and Estimate Continuous Clear-Sky Downwelling LW

The k and humidity factor coefficients are fit to known clear-sky data for three periods separately each day — daylight, sunset to midnight, and midnight to sunrise. When there are sufficient clear periods from

either the SW or LW clear-sky detection found during one of those three periods in a day, the lapse rate constant coefficients are fitted to the data.

Interpolation is then performed between clear periods for each of the three segments of the day separately so that nighttime periods are only interpolated through nighttime fits, etc. Further interpolation is done over the periods of midnight, sunrise, and sunset in order to avoid discontinuities in the calculations.

When a full set of interpolated coefficients is available for each day and time period, continuous clear-sky estimates are produced for the full data set using the formulas given in Section 4.3.2.

4.4 LW Derived Parameters

Two additional parameters, LW fractional sky cover and cloud radiating temperature, are derived from the LW irradiance measurements and clear-sky estimates. Both should be used with caution as described below. Cloud radiating temperature in particular is considered to be a preliminary derivation and has not been peer reviewed.

4.4.1 LW Fractional Sky Cover

The LW effective sky cover is from a technique developed by Durr and Philipona (2004), but with some adjustments. Durr and Philipona use a climatologically derived and applied formulation for clear-sky effective broadband LW emissivity, whereas those here are derived from surrounding clear-sky data as described in Section 4.3. In addition, Durr and Philipona use a calculation of downwelling LW standard deviation for the hour preceding the time of interest in their sky cover prediction, where here we use a running 21-minute standard deviation centered on the time of interest. The variable is deemed as the "effective LW sky cover" in that the downwelling LW at the surface is insensitive to high and thin clouds; thus the sky cover is essentially most representative of the amount of low and mid-level cloudiness (Long 2004, Long and Turner 2008). The original Durr and Philipona retrieval is in oktas, so their inherent uncertainty is at least 1/8 of sky cover. RADFLUXANAL uses a 7-minute running mean to smooth the results.

The retrieval method uses a look-up table of cloud fraction in oktas from two parameters:

1. Standard deviation of downwelling LW over a 21-minute period centered on minute of interest
2. Cloud-free index (CFI) $CFI = \frac{\varepsilon_A}{\varepsilon_C}$, where ε_A = the effective all sky emissivity as defined by the Stephan-Boltzmann equation, and ε_C = the clear-sky emissivity as defined in Section 4.3.2.

Thresholds are introduced in CFI using a "z-factor" which incorporates changing conditions to better handle inversions. $z = CFI_{max} - CFI_{cloud-free} = \frac{1}{\varepsilon_C} - 1$. The look-up table from Durr and Philipona (2004) is reproduced in Figure 3. This table is used by our current algorithm.

After the effective LW fractional sky cover is calculated (partial cloud amount [PCA] in Figure 3), a 7-minute smoothing algorithm is applied in the Radiative Flux Analysis to eliminate large artificial jumps in sky cover between oktas.

CFI (x)	Stdev LDR (y), W m^{-2}	PCA, octas
$x \leq 1$	$y \leq 0.5$	0
$x \leq 1$	$0.5 < y \leq 2$	1
$x \leq 1$	$y > 2$	2
$1 < x \leq (1 + az)$	$y \leq 1$	1
$1 < x \leq (1 + az)$	$1 < y \leq 2$	2
$1 < x \leq (1 + az)$	$y > 2$	3
$(1 + az) < x \leq (1 + bz)$	$y \leq 1$	2
$(1 + az) < x \leq (1 + bz)$	$y > 1$	4
$(1 + bz) < x \leq (1 + cz)$	$y \leq 4$	5
$(1 + bz) < x \leq (1 + cz)$	$y > 4$	6
$x > (1 + cz)$	$y > 8$	6
$x > (1 + cz)$	$2 < y \leq 8$	7
$x > (1 + cz)$	$y \leq 2$	8

^aPCA, partial cloud amount; CFI, cloud-free index; Stdev LDR, variability of longwave downward radiation.

Figure 3. Look-up table describing decision tree for LW fractional sky cover. This is Table 3 in Durr and Phillipona (2004). Here $a=0.12$, $b=0.21$, $c=0.38$.

4.4.2 Cloud Radiating Temperature

Cloud field temperature estimates are considered a "work in progress". The method uses the measured and clear-sky estimated LWdn, the LW sky cover amount, and Independent Pixel Approximation arguments to estimate the LW effective radiating ("cloud") temperature. The uncertainty in this estimation is largely driven by the uncertainty associated with the LW effective sky cover. The value generated assumes a single layer of cloudiness covering the "LW sky cover" portion of the sky, and with uniform radiating properties. Thus this value is best described as an "effective cloud field radiating temperature" with all the assumptions that the word "effective" usually implies. Comparisons have shown that for LW sky cover of 50% or more, the retrieved radiating temperatures show remarkable agreement with corresponding IRT measurements. However, the agreement rapidly degrades for LW sky < 50%; thus we limit these retrievals for times when the LW sky cover is > 50%.

The algorithm is based on the Stephan-Boltzmann equation with the difference between clear and cloudy sky downwelling longwave used to calculate the effective cloud field radiating temperature (T_{cld}).

$$T_{cld} = \left[\frac{LW - LW_{clr}}{(1.0 - \epsilon_c)LW_{scv}\sigma} \right]^{0.25}$$

The equation uses the estimated LW clear sky (LW_{clr}), LW fractional sky cover (LW_{scv}), and the effective clear-sky broadband emissivity (ϵ_c) from previous calculations.

5.0 Future Work

Three variables could use additional development in the future. The clear-sky upwelling LW currently only includes measured upwelling LW when the downwelling LW is clear and does not include estimates of clear-sky upwelling LW at all times. A preliminary algorithm exists for estimating clear-sky upwelling LW, but is considered still in development so it is not included in this VAP. It currently does not work over water, snow, or ice surfaces because the thermal mass of water gives a long response time.

The LW fractional sky cover algorithm could be further developed in comparison to the new infrared sky imager to improve accuracy and resolution. Since the Durr and Phillipona (2004) method was developed based on cloud fraction determined by human observers, it only has limited resolution. ARM is working on fielding an infrared sky imager that eventually should provide the data needed to refine the (or even develop a new) approach, similar to how total sky imager data was used to develop the SW sky cover technique (Long et al. 2006).

The cloud field temperature estimates are included and often compare well with infrared thermometer (IRT) estimates, but the algorithm has not been published in a peer-reviewed publication or thoroughly evaluated and is still considered a work in progress. The cloud field base height values are not included as they are still very preliminary and often incorrect as can be seen in Figure 4.

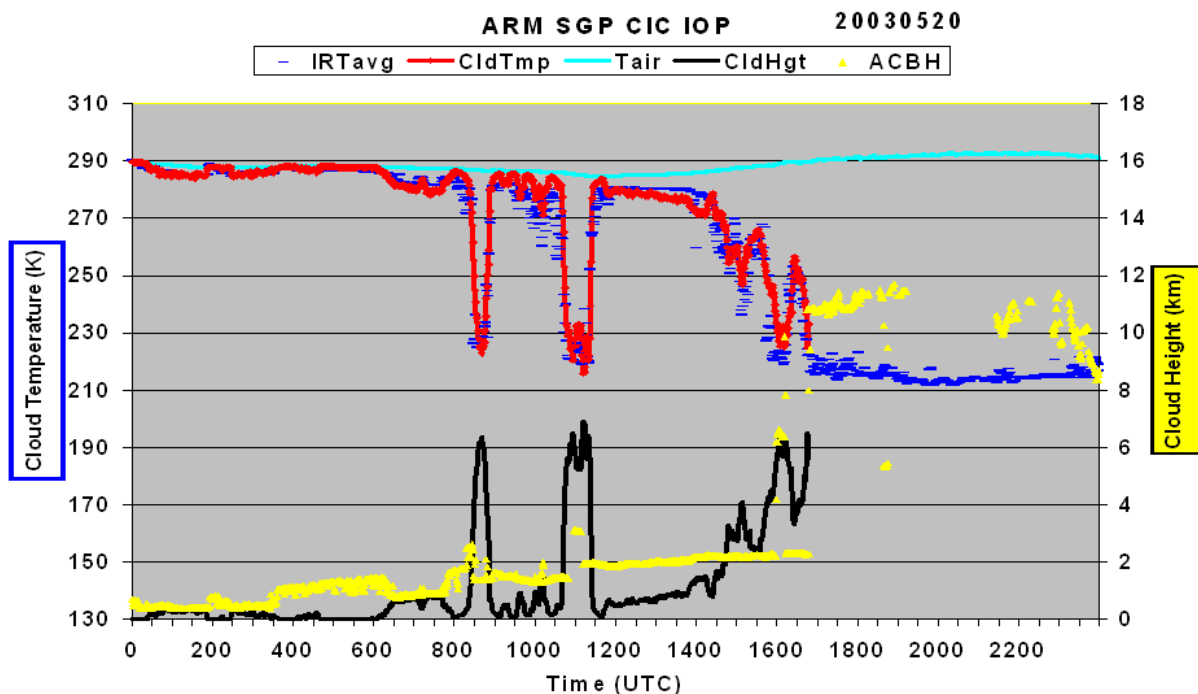


Figure 4. Example of cloud temperature derived from broadband LW measurements (red line) in the RADFLUXANAL VAP compared to the infrared thermometer (blue, IRTavg).

6.0 References

- Barnard, JC, and CN Long. 2004. “A Simple Empirical Equation to Calculate Cloud Optical Thickness Using Shortwave Broadband Measurement.” *Journal of Applied Meteorology and Climatology* 43(7): 1057–1066, [https://doi.org/10.1175/1520-0450\(2004\)043<1057:ASEETC>2.0.CO;2](https://doi.org/10.1175/1520-0450(2004)043<1057:ASEETC>2.0.CO;2)
- Barnard, JC, CN Long, EI Kassianov, SA McFarlane, JM Comstock, M Freer, and GM McFarquhar. 2008. “Development and Evaluation of a Simple Algorithm to Find Cloud Optical Depth with Emphasis on Thin Ice Clouds.” *The Open Atmospheric Science Journal* 2(1): 46–55, <https://doi.org/10.2174/1874282300802010046>
- Brutsaert, W. 1975. “On a derivable formula for long-wave radiation from clear skies.” *Water Resources Research* 11(3): 742–744, <https://doi.org/10.1029/WR011i005p00742>
- Durr, B, and R Philipona. 2004. “Automatic cloud amount detection by surface longwave downward radiation measurements.” *Journal of Geophysical Research – Atmospheres* 109(D5): D05201, <https://doi.org/10.1029/2003JD004182>
- Dutton, EG, JJ Michalsky, T Stoffel, BW Forgan, J Hickey, DW Nelson, TL Alberta, and I Reda. 2001. “Measurement of broadband diffuse solar irradiance using current commercial instrumentation with a correction for thermal offset errors.” *Journal of Atmospheric and Oceanic Technology* 18(3): 297–314, [https://doi.org/10.1175/1520-0426\(2001\)018<0297:MOBDSI>2.0.CO;2](https://doi.org/10.1175/1520-0426(2001)018<0297:MOBDSI>2.0.CO;2)
- Fu, Q. 1996. “An accurate parameterization of the solar radiative properties of cirrus clouds for climate models.” *Journal of Climate* 9(9): 2058–2082, [https://doi.org/10.1175/1520-0442\(1996\)009<2058:AAPOTS>2.0.CO;2](https://doi.org/10.1175/1520-0442(1996)009<2058:AAPOTS>2.0.CO;2)
- Long, CN, and TP Ackerman. 2000. “Identification of clear skies from broadband pyranometer measurements and calculation of downwelling shortwave cloud effects.” *Journal of Geophysical Research – Atmospheres* 105(D12) 15609–15626, <https://doi.org/10.1029/2000JD900077>
- Long, CN, and KL Gaustad. 2004. The Shortwave (SW) Clear-Sky Detection and Fitting Algorithm: Algorithm Operational Details and Explanations. U.S. Department of Energy. DOE/SC-ARM-TR-004.1, http://www.arm.gov/publications/tech_reports/arm-tr-004.1.pdf
- Long, CN. 2004. “The Next-Generation Flux Analysis: Adding Clear-sky LW and LW Cloud Effects, Cloud Optical Depths, and Improved Sky Cover Estimates.” In *Proceedings of the 14th ARM Science Team Meeting*, Albuquerque, New Mexico, <https://pdfs.semanticscholar.org/147a/057a176f0869fa9b33d32af9aa6d5acb8298.pdf>
- Long, CN. 2005. “On the Estimation of Clear-Sky Upwelling Shortwave and Longwave.” In *Proceedings of the 15th ARM Science Team Meeting*, Daytona Beach, Florida, <http://citeseerx.ist.psu.edu/viewdoc/download?doi=10.1.1.298.4013&rep=rep1&type=pdf>
- Long, CN, TP Ackerman, KL Gaustad, and JNS Cole. 2006. “Estimation of fractional sky cover from broadband shortwave radiometer measurements.” *Journal of Geophysical Research – Atmospheres* 111(D11): D11204, <https://doi.org/10.1029/2005JD006475>

Long, CN, and Y Shi. 2006. The QCRad Value Added Product: Surface Radiation Measurement Quality Control Testing, Including Climatologically Configurable Limits. U.S. Department of Energy. DOE/SC-ARM-TR-074, https://www.arm.gov/publications/tech_reports/doe-sc-arm-tr-074.pdf

Long, CN, and Y Shi/ 2008. “An Automated Quality Assessment and Control Algorithm for Surface Radiation Measurements.” *The Open Atmosphere Science Journal* 2: 23–37, <https://doi.org/10.2174/1874282300802010023>

Long, CN, and DD Turner. 2008. “A method for continuous estimation of clear-sky downwelling longwave radiative flux developed using ARM surface measurements.” *Journal of Geophysical Research – Atmospheres* 113(D18): D18206, <https://doi.org/10.1029/2008JD009936>

Marty, C, and R Philipona. 2000. “The clear-sky index to separate clear-sky from cloudy-sky situations in climate research.” *Geophysical Research Letters* 27(17): 2649–2652, <https://doi.org/10.1029/2000GL011743>

Min, Q, and LC Harrison. 1996. “Cloud properties derived from surface MFRSR measurements and comparison with GOES results at the ARM SGP Site.” *Geophysical Research Letters* 23(13): 1641–1644, <https://doi.org/10.1029/96GL01488>

Press, WH, BP Flannery, SA Teukolsky, and WT Vetterling. 1986. *Numerical Recipes: The Art of Scientific Computing*. Cambridge University Press, New York, New York.

Younkin, K, and CN Long. 2003. Improved Correction of IR Loss in Diffuse Shortwave Measurements: An ARM Value-Added Product. U.S. Department of Energy. DOE/SC-ARM-TR-009, https://www.arm.gov/publications/tech_reports/arm-tr-009.pdf



U.S. DEPARTMENT OF
ENERGY

Office of Science